Cerenkov third-harmonic generation via cascaded $\chi^{(2)}$ processes in a periodic-poled $LiTaO_3$ waveguide

Changdong Chen,[1] Jun Lu,[1] Yanhua Liu,[1] Xiaopeng Hu,[1,2] Lina Zhao,[1] Yong Zhang,[1,3] Gang Zhao,[1] Ye Yuan,[1] and Shining Zhu[1]

[1]*National Laboratory of Solid State Microstructures, Nanjing University, Nanjing, 210093 China*

[2]*e-mail: xphu@nju.edu.cn*

[3]*e-mail: zhangyong@nju.edu.cn*

Received November 19, 2010; revised January 17, 2011; accepted February 23, 2011;
posted March 7, 2011 (Doc. ID 138479); published March 28, 2011

We report a type of quasi-phase-matched (QPM) Cerenkov third-harmonic generation (CTHG) in a periodic-poled $LiTaO_3$ waveguide. The CTHG results from a guided-to-guided second-harmonic generation cascaded with a guided-to-radiated sum-frequency generation (SFG) in the waveguide. In the guided-to-radiated SFG process, nonlinear interactions with participating and nonparticipating reciprocal vectors would lead to different CTHG radiations. In addition, the power and temperature detuning characters of QPM CTHG were studied. Theoretical predictions were in good agreement with experimental results.

OCIS codes: 190.0190, 190.2620, 230.7390, 350.5610.

As is known, in nonlinear optical waveguides, when the phase velocity ($\vec{v}_p$) of the nonlinear polarization wave driven by the incident light field is faster than that of the harmonic ($\vec{v}'$), nonlinear Cerenkov radiation (NCR) occurs via a second-order nonlinear process [1–5]. There are mainly two types of phase-matching configurations for NCR, the direct Cerenkov configuration and the quasi-phase-matched (QPM) Cerenkov configuration. Previous experimental and theoretical investigations on QPM Cerenkov radiations [6–8], such as second-harmonic generation (SHG) and sum-frequency generation (SFG), revealed that the QPM Cerenkov configuration has the advantages of high efficiency, wide phase-matching bandwidth, and large tolerance of variations in pump wavelength and waveguide parameters. In a nonlinear waveguide, Cerenkov third-harmonic generation (CTHG) can take place as well [9]. For the realization of CTHG, two possible schemes can be adopted: one is direct CTHG via a $\chi^{(3)}$ process and the other bases on two cascaded $\chi^{(2)}$ processes. Considering the rather small $\chi^{(3)}$ of $LiTaO_3$ (LT), which is about 10^{-8} of its $\chi^{(2)}$, it is preferable to use the cascaded $\chi^{(2)}$ configuration, which comprises the cascaded second-order nonlinear interactions of a guided-to-guided SHG process and a guided-to-radiated SFG process. The fundamental and the generated second harmonic (SH) are guided waves in the waveguide while the third harmonic (TH) is radiated toward the substrate. Up to now, there have been no reports on the experimental realization of CTHG in a nonlinear waveguide.

In this Letter, we present the experimental results of CTHG via two cascaded $\chi^{(2)}$ procedures in a periodic-poled LT (PPLT) planar waveguide. Both of the forward and backward reciprocal vectors could be involved in the interactions. The power and temperature tuning curves of the TH radiations were also explored.

In our experiment, a z-cut LT wafer with a thickness of 0.5 mm and a length of 13 mm was first periodically poled by the electrical poling technique at room temperature, which formed a domain period of $\Lambda = 14.58\,\mu$m and a reversal factor of ~37%. Then, the poled sample was immersed into benzoic acid and proton-exchanged for 6 h at 220 °C. Subsequently, the sample was subjected to annealing treatment for 5 h at 380 °C, which could recover the nonlinear coefficient and create a graded-index layer in the waveguide region with about 3.9 μm depth [10]. The end faces of the waveguide were polished for optical measurement.

The schematic experimental setup is shown in Fig. 1. The fundamental source is a laser diode end-pumped Q-switched $Nd:YVO_4$ laser operating at 1342 nm with a pulse width of ~50 ns. The pulse repetition rate is adjustable within a range of 1–50 kHz. Because a proton-exchanged z-cut LT waveguide only maintains TM modes, the z-polarized IR beam was focused into the waveguide by a cylindrical lens with a focal length of 5 mm. The generated Cerenkov radiations were projected onto a screen placed 110 mm away from the output facet of the sample. A filter M_1 was used to filter out the residual IR beams. The sample was placed on an oven with a controlling accuracy of 0.1 °C.

In the experiment, the repetition rate was set to 5 kHz. The fundamental power was first set to 500 mW and the crystal temperature was kept at 120 °C. A pattern composed of two red (labeled 2 and 4) and four blue spots (labeled 1, 3, 5, and 6) appeared on the screen, as shown in Fig. 2(a). Both of the red spots resulted from Cerenkov SHG of the TM_0 mode at 1342 nm [6]. To give the interpretation for the generation of all the blue spots, we can introduce QPM CTHG, which consists of the cascaded SHG and SFG. In the SHG process, a guided SH mode was generated in the waveguide. The conversion efficiency of SHG was greatly enhanced by the reciprocal vectors of PPLT, which provided enough SH waves to carry out the cascaded guided-to-radiated SFG process. Next, we focused our discussions on the SFG process. As

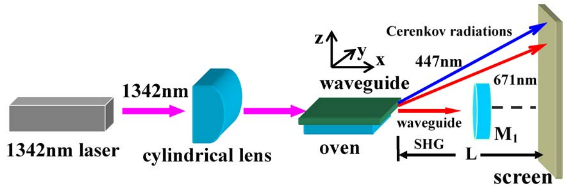

Fig. 1. (Color online) Simplified layout of the experimental setup.

0146-9592/11/071227-03$15.00/0

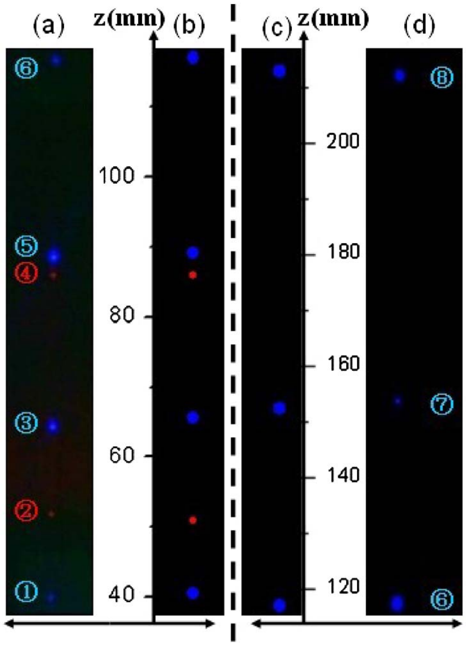

Fig. 2. (Color online) Projection of the radiated Cerenkov SHG (two red spots, 2 and 4) and QPM Cerenkov THG (four blue spots, 1, 3, 5, and 6) at an input power of 500 mW and (a) the calculated distribution of all the spots on the (b) screen. (d) Projection of QPM Cerenkov THG with higher-order backward reciprocal vectors involved at an input power of 600 mW and the (c) simulations of their positions.

shown in Fig. 2(a), the blue spot 3 located between the two red dots resulted from a type of CTHG, in which no reciprocal vector was involved. The phase-matching condition can be written as

$$|\vec{\beta}(\omega)+\vec{\beta}(2\omega)| = |\vec{k}(3\omega)|\cos\theta_1, \tag{1}$$

where $\vec{\beta}(\omega)$ and $\vec{\beta}(2\omega)$ are the propagation constants of the TM_0 modes at 1342 and 671 nm, respectively, $\vec{k}(3\omega) = n_e(3\omega)\vec{k}_0(3\omega)$ is the wave vector of the TH in the substrate, $n_e(3\omega)$ is the extraordinary refractive index of the TH in the substrate, $\vec{k}_0$ is the free space wave vector, and θ_1 is the Cerenkov angle.

In QPM CTHG, the guided-to-radiated SFG process can occur either with or without reciprocal vectors. For the case of participating reciprocal vectors, the phase-matching condition could be expressed as

$$|\vec{\beta}(\omega)+\vec{\beta}(2\omega)+\vec{G}_m| = |\vec{k}(3\omega)|\cos\theta_2, \tag{2}$$

where $G_m = m\frac{2\pi}{\Lambda}$ is the mth reciprocal vector of the periodic structure. When $m=1$, i.e., the first-order forward reciprocal vector becomes involved, $\vec{v}_p$ of the nonlinear polarization wave decreased. The corresponding TH radiation, labeled as spot 1 in Fig. 2(a), would emit along a smaller angle compared with the nonreciprocal vector involved in TH spot 3. Besides forward reciprocal vectors, backward reciprocal vectors ($m = -1, -2\ldots$) could become involved in the radiations as well. As the role of backward reciprocal vectors, $\vec{v}_p$ of the nonlinear polarization wave was accelerated so that the corresponding Cerenkov TH radiations would emit at larger angles.

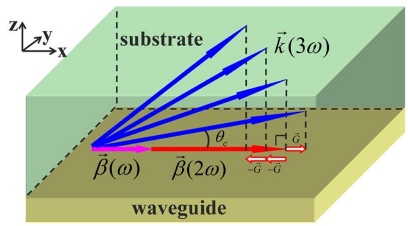

Fig. 3. (Color online) The phase-matching geometry of Cerenkov THG without any reciprocal vectors and with reciprocal vectors $\vec{G}_1$, $\vec{G}_{-1}$, and $\vec{G}_{-2}$.

As shown in Fig. 2(a), blue spots 5 and 6, induced by the first- and second-order backward reciprocal vectors $\vec{G}_{-1}$ and $\vec{G}_{-2}$, respectively, were in a higher position on the screen. The geometries of reciprocal vectors involved and noninvolved CTHG are shown in Fig. 3.

We then raised the input fundamental power to 600 mW, and more higher-order backward reciprocal vectors involved Cerenkov TH spots were observed. As shown in Fig. 2(d), above spot 6, one can clearly see other two higher blue spots 7 and 8, resulting from backward reciprocal vectors $\vec{G}_{-3}$,$\vec{G}_{-4}$, respectively. They were on top of the screen because the CTHG radiation with a larger participating backward reciprocal vector would emit along a larger angle. However, not all the reciprocal vectors could be involved because NCRs required $\vec{v}_p > \vec{v}'$, and the prerequisite condition could be written as

$$|\vec{\beta}(\omega)+\vec{\beta}(2\omega)+\vec{G}_m| < |\vec{k}(3\omega)|. \tag{3}$$

For the case in our experiment, higher-order forward reciprocal vectors ($m > 1$) could not be utilized in the QPM CTHG. We gathered all the Cerenkov TH power and estimated the efficiency from the fundamental IR power to the TH power to be about 0.05%. As shown in Figs. 2(b) and 2(c), we calculated the positions of all the radiation spots on the screen, which were well in accordance with our experimental results. In addition, Table 1 gives the external angles of all the Cerenkov TH spots with participating and nonparticipating reciprocal vectors, and we can see that the experimental data matches well with theoretical values.

Theoretically, following the coupled-mode theory [7], an approximately analytic expression of the CTHG power $P(3\omega)$ can be deduced via a nondepletion approximation as

$$P(3\omega) \propto P^3(\omega)L^3 {d_{\mathrm{SFG}}}^2\left(\frac{\sin\Delta\beta L}{\Delta\beta L}\right)^2\kappa^2|S|^2 \bullet {d_{\mathrm{SFG}}}^2\,\frac{|\vec{\beta}(\omega)+\vec{\beta}(2\omega)+\vec{G}_m|}{\rho}, \tag{4}$$

where $P(\omega)$ represents the pump power, L is the waveguide length, $\Delta\beta$ is the wave vector mismatch in the SHG

Table 1. Experimental (θ_E) and Theoretical (θ_T) Emission Angles of CTHG

	$\vec{G}_1$	0	$\vec{G}_{-1}$	$\vec{G}_{-2}$	$\vec{G}_{-3}$	$\vec{G}_{-4}$
θ_T	20.1°	30.6°	39.0°	46.8°	54.2°	62.8°
θ_E	19.6°	29.9°	39.1°	46.4°	54.5°	62.7°

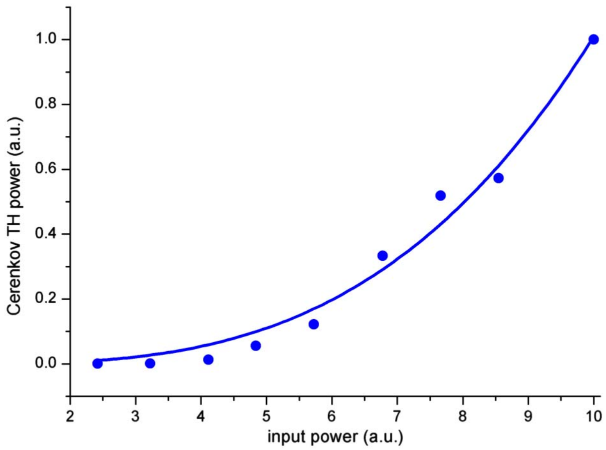

Fig. 4. (Color online) Dependence of Cerenkov TH power on input fundamental power at 1342 nm.

process, κ is the field overlap of the pump and SH waves, S is the field overlap among the pump, SH and Cerenkov TH, d_{SHG} and d_{SFG}, are the effective nonlinear coefficients in the SHG process and the cascading SFG process, respectively, and ρ is the wavenumber of Cerenkov TH. In the experiment, we chose spot 5 associated with $\vec{G}_{-1}$ for the study of the relationship between $P(3\omega)$ and $P(\omega)$. As shown in Fig. 4, $P(3\omega)$ increased with the pump power $P(\omega)$ and the tuning curve was well fitted to be a cubic relationship, which was consistent with the theoretical analysis above. Compared with THG in bulk crystal via cascading $\chi^{(2)}$ processes [11], TH power dependences on the fundamental power and effective nonlinear coefficients are the same as CTHG. The difference between these two cases is the TH power dependence on the interaction length, which follows a biquadratic relation in bulk THG, but a cubic relation in CTHG. The difference lies in the cascading SFG process. For guided-to-radiated SFG, the sum-frequency wave power is proportional to the interaction length [2], while that of conventional SFG in bulk is proportional to the quadratic of the interaction length. The temperature tuning curves for both SH in the waveguide and the radiated TH are shown in Fig. 5. The SH reached its maximum at 117.9 °C with a bandwidth of 3.8 °C, while the CTHG reached the maximum output at 118.1 °C with a bandwidth of 2.3 °C. Unlike THG in bulk QPM materials [12], $P(3\omega)$ increased with the SH power in the waveguide, and both of them obtained the maximum output at nearly the same temperature due to the automatically achieved phase matching in the guided-to-radiated SFG process. Also, it is demonstrated that the other two situations, including the forward reciprocal vector involved and the reciprocal vector noninvolved CTHG, have similar performances, as discussed above.

In conclusion, we reported the experimental realization of CTHG via two cascaded $\chi^{(2)}$ processes in a PPLT planar waveguide. Such a type of CTHG can be modulated by reciprocal vectors, including both forward and backward ones. Different reciprocal vectors of the

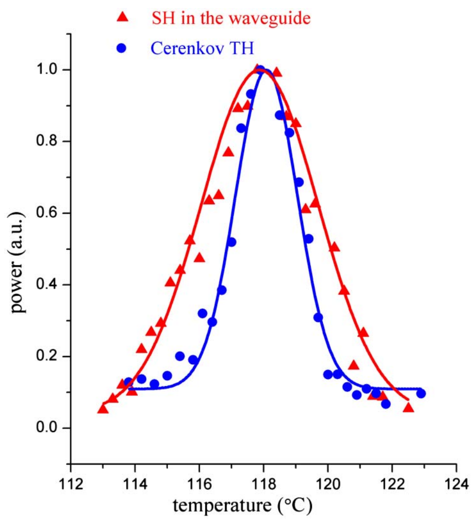

Fig. 5. (Color online) Temperature tuning curves for Cerenkov TH and waveguide SHG.

PPLT would result in different phase velocities of the nonlinear polarization waves and lead to different Cerenkov TH radiation angles. In addition, the power- and temperature-dependent properties of this interaction have also been explored. Theoretical predictions were well in accordance with the experimental results. Further study on coupled nonlinear Cerenkov interactions is in progress.

This work was supported by the National Natural Science Foundation of China (NSFC) under contracts 10904066, 11004097, and 10776011, and the State Key Program for Basic Research of China (contracts 2011CBA00205 and 2010CB630703).

References

1. P. K. Tien, R. Ulrich, and R. J. Martin, Appl. Phys. Lett. **17**, 447 (1970).
2. N. A. Sanford and J. M. Connors, J. Appl. Phys. **65**, 1429 (1989).
3. M. J. Li, M. De Micheli, Q. He, and D. B. Ostrowsky, IEEE J. Quantum Electron. **26**, 1384 (1990).
4. K. Yamamoto, H. Yamamoto, and T. Taniuchi, Appl. Phys. Lett. **58**, 1227 (1991).
5. C. Chen, J. Su, Y. Zhang, P. Xu, X. Hu, G. Zhao, Y. Liu, X. Lv, and S. Zhu, Appl. Phys. Lett. **97**, 161112 (2010).
6. Y. Zhang, Z. D. Gao, Z. Qi, S. N. Zhu, and N. B. Ming, Phys. Rev. Lett. **100**, 163904 (2008).
7. H. Tamada, IEEE J. Quantum Electron. **27**, 502 (1991).
8. M. Vaya, K. Thyagarajan, and A. Kumar, J. Opt. Soc. Am. B **15**, 1322 (1998).
9. K. Hayata, H. Matsumura, and M. Koshiba, J. Appl. Phys. **70**, 1157 (1991).
10. P. G. Suchoski, T. K. Findakly, and F. J. Leonberger, Opt. Lett. **13**, 1050 (1988).
11. R. Ivanov, K. Koynov, and S. Saltiel, Opt. Commun. **212**, 397 (2002).
12. X. P. Hu, G. Zhao, C. Zhang, Z. D. Xie, J. L. He, and S. N. Zhu, Appl. Phys. B **87**, 91 (2007).